Experiments have shown that thermal fluctuations make proteins somewhat porous, especially to small, nonpolar molecules (*15*). Our analysis supports the concept that the active site of AChE has a particularly porous wall at Trp^{84}, which may be of functional importance. Kinetic energy gained by the catalytic residue His^{440} during hydrolysis may pass by way of the peptide linkage to Gly^{441}, one of the channel residues. This energy might increase the probability of opening, causing an organized sequence of catalysis and channel opening.

REFERENCES AND NOTES

1. J. L. Sussman *et al.*, *Science* **253**, 872 (1991).
2. P. H. Axelsen, M. Harel, I. Silman, J. L. Sussman, *Protein Sci.*, in press.
3. M. Harel *et al.*, *Proc. Natl. Acad. Sci. U.S.A.* **90**, 9031 (1993).
4. D. R. Ripoll, C. H. Faerman, P. H. Axelsen, I. Silman, J. L. Sussman, *ibid.*, p. 5128.
5. R. C. Tan, T. N. Truong, J. A. McCammon, J. L. Sussman, *Biochemistry* **32**, 401 (1993).
6. All Arg, Lys, Asp, Glu, NH_2-terminal, and COOH-terminal groups were assigned "ionized" (except Glu^{443}). The Glu^{443} residue was assigned "neutral" (OE2 protonated) because it is fully desolvated and appears to form only two to three hydrogen bonds. All Tyr and Cys side chains were set neutral. Histidine protonation sites were His^{3}, ND1; His^{26}, ND1; His^{159}, NE2; His^{181}, ND1, NE2; His^{209}, NE2; His^{264}, ND1; His^{362}, ND1; His^{398}, ND1; His^{406}, ND1, NE2; His^{425}, ND1, NE2; His^{440}, ND1; His^{471}, ND1, NE2; His^{486}, NE2; and His^{513}, ND1, NE2. The net charge per monomer was −5. Both monomers were assigned identical protonation states. Polar hydrogens were added with the ARGOS package (*17*).
7. With only crystallographic solvent included, the energy was minimized with respect to hydrogen positions for 200 steepest descent steps. The energy was then minimized for 200 steepest descent steps with respect to the coordinates of residues 535 to 537 and 1072 to 1074 to form the COOH-terminal disulfide bond. A pre-equilibrated box of waters [SPC/E model (*18*)] was overlayed repeatedly on the system to fill in a 40 Å sphere centered on atom NE2 of the catalytic His^{440}. The 142 crystallographic waters were retained. Waters closer than 2.5 Å to any crystallographic heavy atom were rejected. Atoms more than 35 Å from His^{440} NE2 were fixed in space for all subsequent calculations to create a constant-volume dynamical system containing 5252 protein atoms and 3117 water molecules. Energy was minimized with respect to water coordinates for 200 steepest descent steps. Then MD on water only was performed for 20 ps, with velocity reassignment at 300 K every 0.2 ps and velocity rescaling (*19*) with time constant 0.2 ps. Energy was then minimized with respect to protein coordinates for 200 steepest descent steps. MD on the protein only was performed for three segments of 5 ps each, with velocity reassignment every 0.2 ps and rescaling with time constant 0.1 ps, at 100 K, 200 K, and 300 K, respectively. Before production calculations were made, MD was used to equilibrate the entire system for 20 ps at 300 K, with separate solute and solvent velocity rescaling with time constant 0.2 ps. During the first 20 ps of production, coordinates were stored every 20 steps. Subsequently, coordinates were stored every five steps. All interactions in a short-range (10 Å) pair list were updated every five steps, while all interactions in a long-range pair list were updated every five steps. Separate solvent-solvent, solvent-solute, and solute-solute pair lists were updated every 10, 15, and 20 steps, respectively. Pair lists were based on charge groups. SHAKE (*20, 21*) was used to constrain bond lengths, permitting the use of a 2-fs time step. All calculations were made with the ARGOS program package (*17*), with GROMOS atomic parameters (*22*). System temperatures approximated 301 K, with solute temperatures of about 298 K and solvent temperatures of about 302 K. Total system potential energy averaged -200×10^3 kJ mol^{-1}, with a drift of −8.0 kJ mol^{-1} ps^{-1} during the final 100 ps. During the final 100 ps, the rms atomic position deviation from crystal coordinates of nonhydrogen atoms in the innermost 25 Å of the simulation sphere averaged 1.7 Å, with a residual upward slope of 0.001 Å ps^{-1}.
8. B. Lee and F. M. Richards, *J. Mol. Biol.* **55**, 379 (1971).
9. Surface generation started with 100 surface points per atom, representing possible locations of the center of a solvent probe sphere. For simplicity, hydrogen atoms were excluded, and all heavy atoms were assigned a radius of 1.8 Å. Two surface points were assigned to the same surface subset if they were closer than the greatest distance between any point and its nearest neighbor on the initial 100-point surface sphere of each atom.
10. C. Weise *et al.*, *EMBO J.* **9**, 3885 (1990).
11. M. Vigny, S. Bon, J. Massoulié, F. Leterrier, *Eur. J. Biochem.* **85**, 317 (1978).
12. S. Englander and N. Kallenbach, *Q. Rev. Biophys.* **16**, 521 (1984).
13. We used the finite-difference Poisson-Boltzmann method (*23*), implemented in the program UHBD (*24*) to compute electrostatic fields in and around AChE. Finite-difference Poisson-Boltzmann calculations were made with protein and solvent dielectric constants of 2 and 80, respectively, physiologic ionic strength (150 mM), and a 2.0 Å Stern layer. The dielectric boundary was defined as the Richards (*25*) probe-accessible surface. The only source charges were the formally charged groups of the molecular dynamics calculation. We used a 65 by 65 by 65 point grid with 1.5 Å spacing.
14. M. Cygler *et al.*, *Protein Sci.* **2**, 366 (1993).
15. A. P. Demchenko, *Essays Biochem.* **22**, 120 (1986).
16. GRASP, vers. 1.04; A. Nicholls and B. Honig, Columbia University, New York.
17. T. P. Straatsma and J. A. McCammon, *J. Comput. Chem.* **11**, 943 (1990).
18. H. J. C. Berendsen, J. R. Grigera, T. P. Straatsma, *J. Phys. Chem.* **91**, 6269 (1987).
19. H. J. C. Berendsen, J. P. M. Postma, W. F. van Gunsteren, A. DiNola, J. R. Haak, *J. Chem. Phys.* **81**, 3684 (1984).
20. W. F. van Gunsteren and H. J. C. Berendsen, *Mol. Phys.* **34**, 1311 (1977).
21. J.-P. Ryckaert, G. Ciccotti, H. J. C. Berendsen, *J. Comput. Phys.* **23**, 327 (1977).
22. W. F. van Gunsteren and H. J. C. Berendsen, *Groningen Molecular Simulation* (GROMOS) *Library Manual* (Biomos, Groningen, Netherlands, 1987).
23. J. Warwicker and H. C. Watson, *J. Mol. Biol.* **157**, 671 (1982); I. Klapper, R. Hagstrom, R. Fine, K. Sharp, B. Honig, *Proteins Struct. Func. Gen.* **1**, 47 (1986); M. K. Gilson, K. A. Sharp, B. H. Honig, *J. Comput. Chem.* **9**, 327 (1988).
24. M. E. Davis, J. D. Madura, B. A. Luty, J. A. McCammon, *Comput. Phys. Commun.* **62**, 187 (1991).
25. F. M. Richards, *Annu. Rev. Biophys. Bioeng.* **6**, 151 (1977).
26. Atomic coordinates for the open back door conformation are available by anonymous Internet file transfer program (ftp) to mrbun.chem.uh.edu.

We thank B. Honig and A. Nicholls for making available the graphics program GRASP and R. Gillilan and H. S. R. Gilson for helpful discussions. Supported by the Robert A. Welch Foundation, the National Institutes of Health, the National Science Foundation, the Grand Challenge Program of the National Science Foundation supercomputer centers, the Minerva Foundation, the Kimmelman Center, and U.S. Army Medical Research and Development Command Contract no. DAMD17-93-C-3070. M.K.G. is a Howard Hughes Physician Research Fellow and I.S. is Bernstein-Mason Professor of Neurochemistry. P.H.A. is supported by the Markey Charitable Trust.

10 August 1993; accepted 15 November 1993

Suppression of Ras-Induced Transformation of NIH 3T3 Cells by Activated $G\alpha_s$

Jianghao Chen and Ravi Iyengar*

Conversion of external signals into proliferative responses may be mediated by interactions between signaling pathways that control cell proliferation. Interactions between $G\alpha_s$, the α subunit of the heterotrimeric guanine nucleotide binding protein that stimulates adenylyl cyclase, and Ras, an important element in growth factor signaling, were studied. Expression of activated $G\alpha_s$ in NIH 3T3 cells increased intracellular concentrations of adenosine 3′,5′-monophosphate (cAMP) and inhibited H-Ras–stimulated DNA synthesis and mitogen-activated protein kinase activity. Activated $G\alpha_s$ and 8-Br-cAMP suppressed H-Ras–induced transformation of NIH 3T3 cells. Apparently, $G\alpha_s$ inhibits proliferative signals from Ras by stimulating cAMP production and activating protein kinase A.

Many heterotrimeric guanine nucleotide binding proteins (G proteins) participate in mitogenic signaling (*1*). Of these, the G_s and its signaling pathway are probably the most enigmatic. In a few systems, receptor activation of the cAMP pathway is mitogenic (*2*), but in most systems raising the intracellular concentration of cAMP has no effect on cell proliferation. An activated mutant form of $G\alpha_s$ has been identified in pituitary tumors and postulated to be an oncogene (*3*), but has not been shown to transform cells in vitro. Thus $G\alpha_s$ might not produce a strong proliferative signal by itself, but it might have effects in conjunc-

J. Chen, Department of Biochemistry, Mount Sinai School of Medicine, City University of New York, NY 10029, USA.
R. Iyengar, Department of Pharmacology, Mount Sinai School of Medicine, City University of New York, One Gustave L. Levy Place, New York, NY 10029, USA.

*To whom correspondence should be addressed.

tion with other proliferative signals. Ras functions as a downstream element of several growth factor receptor tyrosine kinases (*4*). Both Ras and $G\alpha_s$ belong to the guanosine triphosphatase (GTPase) superfamily and can be converted to their active forms by mutations that block their intrinsic GTPase activities (*5*). We used such mutated forms to test the effects of expression of activated $G\alpha_s$ on H-Ras–induced proliferation and transformation of NIH 3T3 cells.

$G\alpha_s$, in which Gln 227 was changed to Leu (Q227L), was prepared by site-directed mutagenesis (*6*). We transfected NIH 3T3 cells with wild-type $G\alpha_s$, Q227L $G\alpha_s$ (α_s*) in the vector pMam-Neo (pMN), or vector alone. Selected cells were individually plated, and several clonal lines were established (*7*). Expression of the insert was induced by addition of dexamethasone and monitored by measurement of cAMP. Two NIH 3T3 clones that have a 60 to 100% increase in basal cellular concentrations of cAMP were used for further studies. We determined the effect of expression of α_s* on H-Ras–stimulated mitogenesis (*8*) and mitogen-activated protein (MAP) kinase activity. Expression of α_s* did not alter the rate of DNA synthesis as assessed by [^{3}H]thymidine incorporation. Cells transfected with an H-*ras*–containing plasmid (pT24) showed a fivefold increase in the rate of DNA synthesis. Expression of α_s* suppressed H-Ras–induced DNA synthesis (Fig. 1A). The mitogenic signal from Ras is transmitted through the MAP kinase pathway (*9*). We therefore determined the effect of expression of α_s* on H-Ras–induced MAP kinase activity (*10*). Expression of α_s* suppressed H-Ras–stimulated MAP kinase activity by about 50%, similar to its effect on DNA synthesis (Fig. 1B).

To establish that the observed reduction of H-Ras–stimulated MAP kinase activity by α_s* was not due to clonal variation, we examined another clonal line expressing α_s*. Both clonal lines expressing α_s* showed increased intracellular concentrations of cAMP as compared to those of vector-transfected lines. Both lines also showed a 50% reduction in H-Ras–stimulated MAP kinase activity as compared to that of the control cell line (Table 1).

Because H-Ras–induced mitogenesis leads to transformation of NIH 3T3 cells, we tested if the expression of α_s* affected the Ras-induced transformation of NIH 3T3 cells (*11*). Expression of α_s* resulted in an almost total blockade of H-Ras–induced transformation at all concentrations of H-Ras plasmid tested (Fig. 2A). Transfection efficiencies for the various clonal lines were very similar (*12*). To determine if the transfected H-Ras was expressed in similar amounts in both control and α_s*-expressing cells, we labeled proteins with [^{35}S]methionine and immunoprecipitated H-Ras with a

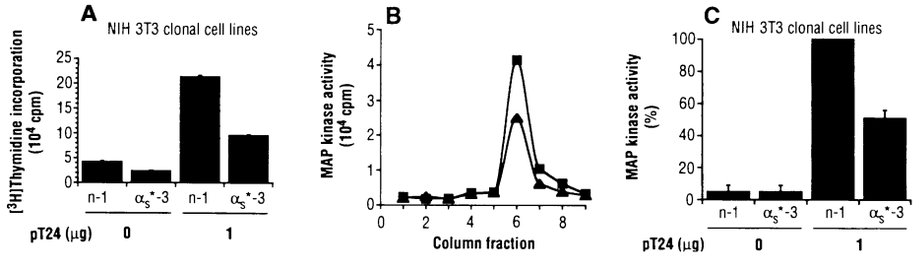

Fig. 1. Effects of expression of mutant activated $G\alpha_s$ on H-Ras–induced mitogenesis (**A**) and MAP kinase activity (**B** and **C**). Clonal NIH 3T3 lines n-1 and α_s*-3 were derived from cells transfected with pMAM-neo and pMAM-neo-α_s*, respectively. The α_s*-3 line expressed α_s* when treated with dexamethasone. These cell lines were transfected with or without H-*ras* plasmid (pT24) and grown for 2 weeks, with dexamethasone added on alternate days. The cells were split on every third day. After the 2-week period, the cells were plated in 24-well plates and incorporation of [^{3}H]thymidine was measured. (A) Values are means of triplicate determinations. The results of one representative of four experiments are shown. (B and C) Cells (4×10^6 per 100-mm plate) were incubated for 20 hours with DMEM without serum but with bovine serum albumin (0.1%) to achieve quiescence. The cells were then extracted and MAP kinase activity was measured (*10*). (B) Column profiles of H-Ras–stimulated MAP kinase activity (in a .20-μl portion of column eluate) from control (■) and α_s*-expressing (▲) clonal lines in one experiment. (C) A summary of four separate experiments. Values are means ± SD.

Table 1. Accumulation of cAMP and MAP kinase activity in NIH 3T3 clonal cell lines expressing mutant activated $G\alpha_s$.

Cell lines	cAMP	MAP kinase activity
n-1	0.95 ± 0.05	4.80
α_s*-3	1.58 ± 0.16	2.84
α_s*-14	2.02 ± 0.21	2.47

For the cAMP measurements, the clonal cells were treated with dexamethasone (1 μM) on alternate days for 1 week. The cells were then labeled with [^{3}H]adenine (2 μCi/ml) for 24 hours. Accumulation of cAMP was measured for 30 min in the presence of 1-methyl-3-isobutylxanthine (1 mM). Cells were extracted in trichloroacetic acid (5%), adenosine triphosphate (1 mM) and cAMP (1 mM). [^{3}H]cAMP and [^{3}H]ATP were separated by sequential chromatography on Dowex-50 and neutral alumina. cAMP accumulation is expressed as [^{3}H]cAMP/([^{3}H]cAMP + [^{3}H]ATP) × 10^3. Values are means ± SD of triplicate determinations. MAP kinase activity was assayed 2 weeks after transfection with H-*ras* plasmid (1 μg) as described (Fig. 1B). The MAP kinase activities are expressed as CPM/15 min/1 μg of cellular protein × 10^{-3}. As the MAP kinase activities are the sum of several fractions that comprise the peak, no error estimates could be obtained. The lines used were n-1, a clonal line derived from cells transfected with pMAM-neo, and α_s*-3 and α_s*-14, clonal lines derived from cells transfected with pMAM-neo-α_s*.

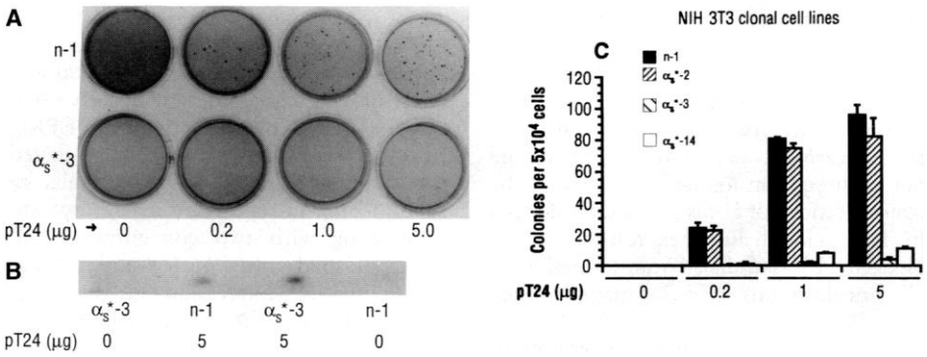

Fig. 2. Effects of α_s* on H-Ras–induced transformation of NIH 3T3 cells. (**A**) Soft agar plates of cells from the clonal lines n-1 and α_s*-3 transfected with the indicated amounts of H-*ras* plasmid (pT24) by the calcium phosphate method. The transfected cells were treated with dexamethasone (1 μM) to induce expression of α_s* and then plated onto soft agar to assess colony formation. (**B**) Immunoprecipitation of Ras proteins extracted from NIH-3T3 cell lines, n-1 and α_s*-3, that were cotransfected with genomic NIH 3T3 DNA (20 μg) and pRSV 1.1 (1 μg) with or without H-*ras* plasmid (5 μg). The cells were cultured, labeled, and extracted. Ras was immunoprecipitated as described (*13*). (**C**) Several NIH 3T3 cell lines were transfected with various amounts of H-*ras* plasmid as indicated. The ability of transfected cells to form colonies in soft agar was determined. NIH 3T3 cells used were n-1, a vector-containing cell line; α_s-2, a cell line expressing exogenous wild-type $G\alpha_s$; α_s*-3 and α_s*-14, cell lines expressing the mutant activated $G\alpha_s$. Values are means ± SD of triplicate plates. The experiment in each panel is representative of three experiments except the immunoblotting, which was only done twice.

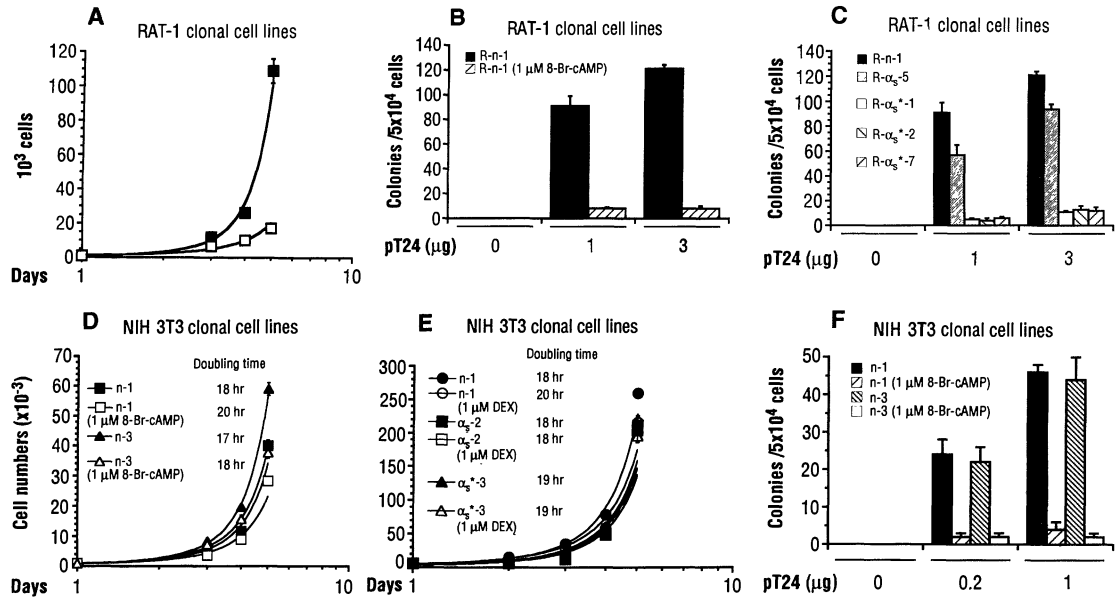

Fig. 3. Effects of 8-Br-cAMP on mitogenesis and H-Ras–induced transformation of RAT-1 and NIH 3T3 lines. (**A**) Cells were seeded into 24-well plates (1 × 10^3 cells per well) in DMEM (1 ml) with bovine calf serum (10%) and grown in the presence (□) or absence (■) of 8-Br-cAMP (1 μM). Each group included four wells. The number of cells was determined on days 3, 4, and 5 (*22*). (**B**) The clonal line R-n-1 was grown overnight in the presence of 8-Br-cAMP (1 μM) and transfected without or with the indicated concentrations of H-*ras* plasmid. After transfections, the cells were cultured for 4 days with dexamethasone treatment on alternate days before plating on soft agar plates. Values are means ± SD of triplicate plates. (**C**) Several clonal lines of RAT-1 cells were transfected with various amounts of H-*ras* plasmid as indicated. The ability of transfected cells to form colonies in soft agar was determined. The RAT-1 cells used were R-n-1, which contains the vector pMam-neo; R-α_s-5, which expresses exogenous wild-type Gα_s; and R-α_s*-1, R-α_s*-2, and R-α_s*-7, which express mutant activated α_s. Values are means ± SD of triplicate plates. (**D**) Cells from NIH 3T3 lines n-1 and n-3 were seeded into 24-well plates (1 × 10^3 cells per well) in DMEM (1 ml) with bovine calf serum (10%) and were grown in the presence or absence of 1 μM 8-Br-cAMP. In another experiment (**E**) n-1, α_s-2, and α_s*-3 cells (6 × 10^3 cells per well) were grown in the presence or absence of dexamethasone (1 μM). Each group included four wells. The numbers of cells were determined on the indicated days (*22*). (**F**) The clonal lines n-1 and n-3 were grown overnight in the presence of 8-Br-cAMP (1 μM) and transfected without or with indicated concentrations of H-*ras* plasmid. After transfections, the cells were cultured for 1 day in the presence of dexamethasone (1 μM) before plating on soft agar plates. Values are means ± SD of triplicate plates. The experiment in each panel is representative of three experiments.

monoclonal antibody to Ras, Y13-259 (*13*). Upon transfection with H-ras plasmid, there was an increase in the amount of H-Ras, and expression of α_s* did not affect this increase (Fig. 2B). Therefore, the observed suppression of transformation did not result from suppression of synthesis of H-Ras. We also compared H-Ras–induced transformation of two separate clonal lines expressing α_s* to one expressing exogenous wild-type Gα_s and a control clone transfected with vector only. Expression of exogenous wild-type Gα_s did not increase cellular cAMP concentrations (*12*) and did not suppress transformation at any of the concentrations of H-*ras* plasmid tested, but in both clonal lines expression of α_s* blocked H-Ras–induced transformation at all concentrations of H-Ras plasmid tested (Fig. 2C).

Decreasing the cellular concentrations of cAMP promotes cell division in RAT-1 cells (*14*), but no such effects have been described for NIH 3T3 cells. We tested whether increasing the intracellular concentrations of cAMP or expression of α_s* could suppress mitogenesis in RAT-1 or NIH 3T3 cells. Addition of 8-Br-cAMP suppressed the proliferation of Rat-1 cells (Fig. 3A) and suppressed H-Ras–induced transformation (Fig. 3B). Expression of α_s* also suppressed H-Ras–induced transformation of the RAT-1 lines (Fig. 3C). In contrast, addition of 8-Br-cAMP or expression of α_s* did not affect the proliferation of NIH 3T3 cells (Fig. 3D). However, in two control clonal lines, incubation with 8-Br-cAMP resulted in suppression of H-Ras–induced transformation (Fig. 3E).

To ascertain if α_s* suppressed H-Ras–induced transformation by causing synthesis of cAMP and activation of protein kinase A (PKA), we studied the effect of a dominant negative PKA subunit on the effect of α_s*. The dominant negative regulatory subunit blocks activation of PKA in NIH 3T3 cells (*15*). We cotransfected the dominant negative PKA regulatory subunit or wild-type PKA regulatory subunit along with two concentrations of H-*ras* plasmid into control and α_s*-expressing cells. Expression of dominant negative but not the wild-type PKA completely blocked the suppressive effect of α_s* expression on H-Ras–induced transformation (Fig. 4). These results indicate that the effects of α_s* are mediated through cAMP and PKA.

Ras signaling through the MAP kinase pathway is crucial for proliferative responses (9). Both the duration (*16*) and amplitude of MAP kinase activity may be important factors when MAP kinase activation gets converted into a biological response. In some situations partial inhibition of MAP kinase activity appears to translate into an almost total loss of biological response (Fig. 1) (*17*). It is possible that negative biochemical integration between the signaling pathways may be achieved by lowering the positive signal below the threshold that triggers the bio-

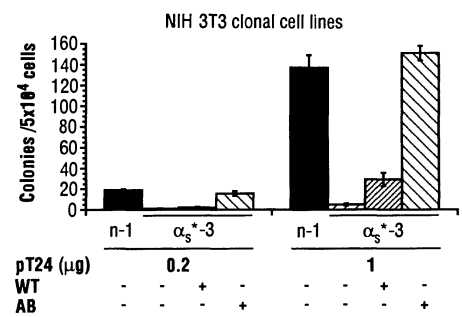

Fig. 4. Effects of the dominant negative PKA regulatory subunit expressed from the plasmid (pHL-REV_{AB}neo, 10 μg) (AB) or control (wild-type PKA regulatory subunit in pHL-REV_{WT}neo, 10 μg) (WT) on H-Ras–induced transformation in NIH 3T3 clonal lines n-1 and α_s*-3. Cells were cotransfected with indicated amounts of H-*ras* plasmid without or with the vectors encoding the PKA regulatory subunits. After transfections, the cells were induced with dexamethasone (1 μM) and plated onto soft agar plates to score for colony formation. Values are means ± SD of triplicate determinations. The result in each panel is representative of three experiments.

logical response. Alternatively, α_s* may inhibit transformation by inhibiting other signaling pathways.

Alteration in cellular concentration of cAMP by itself does not affect regulation of mitogenesis in NIH 3T3 cells or in most other mammalian cell types (*18*). Mutations in *ras* occur commonly in human tumors (*19*). Thus activated Gα_s may suppress transformation of other cell types. Because expression of α_s* only modestly increases the cellular concentrations of cAMP, it is possible that the blockade of transformation by α_s* can be achieved without raising cellular cAMP concentrations to deleterious levels. NIH 3T3 cells are on the verge of transformation (*20*) and can be transformed without the introduction of foreign oncogenes (*21*). The use of such a system heightens the potential significance of our observations by indicating that α_s* can block the transformation of cells that have substantially progressed through the multiple steps involved in neoplastic transformation. Thus targeted implantation of α_s* may be a useful strategy for preventing the development of cancers in some predisposed cells or tissues.

REFERENCES AND NOTES

1. J. Pouyssegur, *Annu. Rev. Physiol.* **54**, 195 (1992); S. Winitz *et al.*, *J. Biol. Chem.* **268**, 19196 (1993); V. J. LaMorte *et al.*, *J. Cell Biol.* **245**, 1146 (1993).
2. J. E. Dumont, J.-C. Jauniaux, P. P. Roger, *Trends Biochem. Sci.* **14**, 67 (1989).
3. C. A. Landis *et al.*, *Nature* **340**, 692 (1989); F. McCormick, *ibid.* **340**, 678 (1989).
4. D. R. Lowy and M. Willumsen, *Annu. Rev. Biochem.* **62**, 851 (1993).
5. H. R. Bourne, D. A. Sanders, F. McCormick, *Nature* **349**, 117 (1991).
6. Q227L Gα_s was prepared by site directed mutagenesis with the polymerase chain reaction (PCR). Briefly, oligonucleotides containing the mutated sequence (638 A→T and 639 G→T) were used to generate a PCR fragment that encodes a Leu residue at position 227 instead of the native Gln. The wild-type Gα_s was digested with Bam HI and the wild-type fragment was replaced with the PCR fragment encoding the mutant sequence. The presence and position of the mutation were verified by DNA sequencing. The wild-type Gα_s and mutant Gα_s were then transferred into the mammalian expression vector pMam-neo (*7*). Individual clonal lines transfected from vector (pMam-neo) alone or vector containing wild-type Gα_s or Q227L Gα_s were isolated by G-418 selection after calcium phosphate transfection as described (*7*).
7. M. DeVivo, J. Chen, J. Codina, R. Iyengar, *J. Biol. Chem.* **267**, 18263 (1992); S. D. Kroll *et al.*, *ibid.*, p. 23183.
8. Cells (10^4 per well) were plated in 24-well plates in 1 ml of Dulbecco's modified Eagles medium (DMEM) containing calf serum (10%) and induced with dexamethasone (1 μM) for 2 days. On the third day, the medium was replaced with fresh medium (1 ml) containing calf serum (1%). On the fourth day, 1 μCi of [^{3}H]thymidine was added along with dexamethasone and the cells were grown for 24 hours. The cells were then washed twice with phosphate-buffered saline. The radioactivity precipitated after incubation of the cells with trichloroacetic acid (5%) was estimated by liquid scintillation counting.
9. J. Marx, *Science* **260**, 1588 (1993); R. J. Davis, *J. Biol. Chem.* **268**, 14553 (1993); J. Blenis, *Proc. Natl. Acad. Sci. U.S.A.* **90**, 5889 (1993).
10. Cells were extracted and the extract was resolved on Mono-Q columns of a fast protein liquid chromatography (FPLC) system. MAP kinase activity in the FPLC fractions was measured with a synthetic peptide containing amino acids 662 to 681 of the epidermal growth factor receptor as substrate [S. K. Gupta *et al.*, *J. Biol. Chem.* **267**, 7987 (1992)].
11. After transfection with the H-*ras* plasmid (pT24), which contains an activated c-H-*ras* oncogene isolated from human T24 bladder carcinoma cells [M. Goldfarb, *et al.*, *Nature* **296**, 404 (1982)], cells were induced for either 1 day (NIH 3T3 cells) or 3 days (RAT-1) with 1 mM dexamethasone before plating on soft agar plates. Procedures for the colony formation assay have been published (*7*). Transfection efficiencies for the various NIH 3T3 clonal lines were very similar (*12*). No differences were found in the transfection efficiencies for the different RAT-1 clonal lines (*12*).
12. J. Chen, thesis, City University of New York (1994).
13. [^{35}S]methionine-labeled H-Ras was immunoprecipitated from extracts of NIH 3T3 cell lines n-1 and α_s*-3, which were cotransfected with 20 μg of genomic NIH 3T3 DNA and 1 μg of pRSV1.1 DNA (a cDNA that confers hygromycin resistance) with or without of H-Ras plasmid (5 μg). After transfection, cells were induced with Dexamethasone (1 μM) for 1 day and grown in medium containing hygromycin B (400 μg/ml). Medium was changed every 3 days. After 1 week, cells were treated with 1 μM of dexamethasone again. One week later, 3 × 10^6 cells were labeled with 0.25 mCi of [^{35}S]methionine for 3 hours. Cells were then lysed, and Ras was immunoprecipitated with monoclonal antibody to Ras, Y13-259 according to the protocol provided by Oncogene Science Inc. The immunoprecipitated products were resolved on SDS-polyacrylamide gels (15%) and visualized by autoradiography.
14. E. J. van Corven, A. Groenink, K. Jolink, T. Eicholta, E. H. Moolenar, *Cell* **59**, 45 (1989).
15. C. H. Clegg, L. A. Correll, G. G. Cadd, G. S. McKnight, *J. Biol. Chem.* **262**, 13111 (1987).
16. S. Traverse, N. Gomez, H. Paterson, C. Marshall, P. Cohen, *Biochem. J.* **288**, 351 (1992).
17. S. J. Cook *et al.*, *EMBO J.* **12**, 3475 (1993).
18. A. Spada, L. Vallar, G. Faglia, *Trends Endocrinol. Metab.* **10**, 355 (1992).
19. M. Barbacid, *Annu. Rev. Biochem.* **56**, 779 (1987).
20. P. W. J. Rigby, *Nature* **297**, 451 (1982).
21. H. Rubin and K. Xu, *Proc. Natl. Acad. Sci. U.S.A.* **87**, 1860 (1989).
22. Doubling times were calculated using the equations $Y = Y_0(e^{kt})$, where Y is the number of cells on a given day, Y_0 is the number of cells on day zero, t is time in days, and k is the calculated rate constant; doubling time = (0.693/k) × 24 hours.

23. We thank R. Krauss for many useful discussions and plasmids and S. McKnight for the wild-type and dominant negative PKA regulatory subunit plasmids. J. C. was supported by a CUNY Dissertation Award Fellowship. Supported by grants from the NIH (CA-44998 and DK-38761) and ACS (CD-518).

14 October 1993; accepted 25 January 1994

Fusion of a Kinase Gene, *ALK*, to a Nucleolar Protein Gene, *NPM*, in Non-Hodgkin's Lymphoma

Stephan W. Morris,* Mark N. Kirstein, Marcus B. Valentine, Kristopher G. Dittmer, David N. Shapiro, David L. Saltman, A. Thomas Look

The 2;5 chromosomal translocation occurs in most anaplastic large-cell non-Hodgkin's lymphomas arising from activated T lymphocytes. This rearrangement was shown to fuse the *NPM* nucleolar phosphoprotein gene on chromosome 5q35 to a previously unidentified protein tyrosine kinase gene, *ALK*, on chromosome 2p23. In the predicted hybrid protein, the amino terminus of nucleophosmin (NPM) is linked to the catalytic domain of anaplastic lymphoma kinase (ALK). Expressed in the small intestine, testis, and brain but not in normal lymphoid cells, ALK shows greatest sequence similarity to the insulin receptor subfamily of kinases. Unscheduled expression of the truncated ALK may contribute to malignant transformation in these lymphomas.

Large-cell lymphomas comprise ~25% of all non-Hodgkin's lymphomas in children and young adults. Approximately one-third of these tumors have a t(2;5)(p23;q35) chromosomal translocation (*1*), which suggests that rearrangement of cellular proto-oncogenes on these chromosomes contributes to lymphomagenesis. Lymphomas with the t(2;5) typically involve lymph nodes, skin, lung, soft tissue, bone, and the gastrointestinal tract and arise predominantly from activated T lymphocytes (*2*). The malignant cells express interleukin-2 (IL-2) receptors and CD30 (Ki-1) antigen, a receptor for a ligand related to tumor necrosis factor (*3*). By the updated Kiel lymphoma classification, most tumors with the t(2;5) are classified as anaplastic large-cell non-Hodgkin's lymphomas (*4*).

To clone the genes altered by the t(2;5), we used a positional strategy that was based

S. W. Morris, M. N. Kirstein, M. B. Valentine, K. G. Dittmer, D. N. Shapiro, A. T. Look, Departments of Experimental Oncology and Hematology-Oncology, St. Jude Children's Research Hospital, Memphis, TN 38105, USA, and Department of Pediatrics, University of Tennessee College of Medicine, Memphis, TN 38163, USA.
D. L. Saltman, Genelabs Inc., Redwood City, CA 94063, USA.

*To whom correspondence should be addressed.